

Article

Multiple time series forecasting using quasi-randomized functional link neural networks

Thierry Moudiki ^{1,*} , Frédéric Planchet ¹ and Areski Cousin ²¹ ISFA, Laboratoire SAF, Université Claude Bernard Lyon I, France

* thierry.moudiki@gmail.com

² Université de Strasbourg, France

Academic Editor: name

Version February 16, 2018 submitted to Risks

Abstract: We are interested in obtaining forecasts for multiple time series, by taking into account the potential nonlinear relationships between their observations. For this purpose, we use a specific type of regression model on an augmented dataset of lagged time series. Our model is inspired from dynamic regression models (Pankratz (2012)), with the response variable's lags included as predictors, and is known as Random Vector Functional Link (RVFL) neural networks. The RVFL neural networks have been successfully applied in the past, to solving regression and classification problems. The novelty of our approach is to apply an RVFL model to multivariate time series, under two separate regularization constraints on the regression parameters.

Keywords: Forecasting; Multivariate time series; Dynamic regression; Neural networks

1. Introduction

In this paper, we are interested in obtaining forecasts for multiple time series, by taking into account the potential nonlinear relationships between their observations. This type of problem has been tackled recently by Exterkate et al. (2016), who applied kernel regularized least squares to a set of macroeconomic time series. The Long Short-Term Memory neural networks (LSTM) architectures (introduced by Hochreiter and Schmidhuber (1997)) are another family of models, which are currently widely used for this purpose. As a basis for our model, we will use (quasi-)randomized neural networks known as Random Vector Functional Link neural networks (RVFL networks hereafter)

The forecasting method described in this paper, provides useful inputs for Insurance quantitative Risk Management models; the interested reader can refer to Bonnin et al. (2015) for example.

To the best of our knowledge, randomized neural networks were introduced by Schmidt et al. (1992), and the RVFL networks were introduced by Pao et al. (1994). An early approach for multivariate time series forecasting using neural networks is described in Chakraborty et al. (1992). They applied a *back propagation* algorithm from Rumelhart et al. (1988) to trivariate time series, and found that the combined training of the series gave better forecasts than a separate training of each individual series. The novelty of the approach described in this paper is to derive an RVFL model for multiple time series, under two separate regularization constraints on the parameters, as it will be described in details in section 2.3.

RVFL networks are *multilayer feedforward* neural networks, in which there is a *direct link* between the predictors and the output variable, aiming at capturing the linear relationships. In addition to the *direct link*, there are new features: the hidden nodes (the dataset is augmented), that help to capture the nonlinear relationships between the time series. These new features are obtained by random

32 simulation over a given interval. More details on the *direct link* and the hidden nodes will be provided
33 in the next section.

34 The RVFL networks have been successfully applied to solving different types of classification and
35 regression problems; see for example [Dehuri and Cho \(2010\)](#). More specifically, they have been applied
36 to univariate time series forecasting by [Ren et al. \(2016\)](#). A comprehensive survey can be found in
37 [Zhang and Suganthan \(2016\)](#); where a large number of model specifications are tested on classification
38 problems, including changing the range of hidden layer's randomization.

39 Here, we will use RVFL networks with one hidden layer. And instead of relying on fully
40 randomized nodes, we will use sequences of deterministic quasi-random numbers. Indeed, with fully
41 randomized nodes, the model fits obtained are dependent on the choice of a simulation *seed*. Typically,
42 a different fitting solution would be obtained for each *seed*.

43 In our various numerical examples from section 3, we will apply the RVFL networks to forecasting
44 trivariate time series, notably (but not only) in a Dynamic Nelson Siegel (DNS) framework (see [Nelson
45 and Siegel \(1987\)](#), [Diebold and Li \(2006\)](#)). We will obtain point forecasts and predictive distributions for
46 the series, and see that in this RVFL framework, one (or more) variable(s) can be stressed, and influence
47 the others. More precisely, about this last point, it means that it is possible, as in dynamic regression
48 models ([Pankratz \(2012\)](#)) to assign a specific future value to one regressor, and obtain forecasts of the
49 remaining variables. Another advantage of the model described here, is its ability to integrate multiple
50 other exogenous variables, without overfitting in-sample data.

51 2. Description of the model

52 The general procedure for obtaining the model's optimal parameters and predictions is
53 summarized in figure 1.

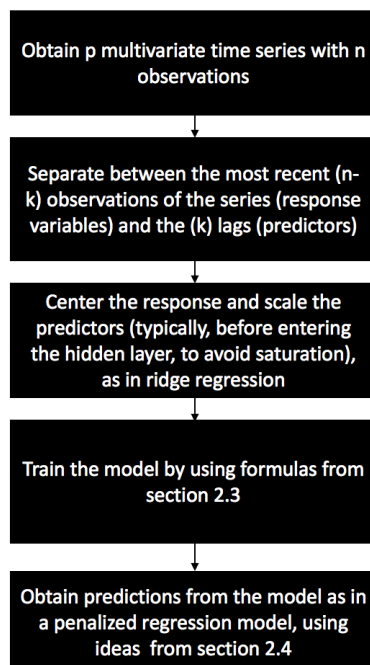


Figure 1

54 This procedure is described in details in the next sections, especially sections 2.3 and 2.4.

55 2.1. On a single layer RVFL networks

We rely on single layer feed forward neural networks (SLFN). Considering that an output variable $y \in \mathbb{R}^n$ is to be explained by a set of observed predictors $Z^{(j)} \in \mathbb{R}^n, j \in \{1, \dots, p\}$, the RVFL networks we will use to explain y can be described for $i \in \{1, \dots, n\}$ as:

$$y_i = \beta_0 + \sum_{j=1}^p \beta_j Z_i^{(j)} + \sum_{l=1}^L \gamma_l g \left(\sum_{j=1}^p W^{(j,l)} Z_i^{(j)} \right) + \epsilon_i$$

56 g is called *activation function*, L is the number of nodes in the hidden layer, $W^{(j,l)}$ are elements of the
 57 hidden layer, and the parameters β_j and γ_l are to be learned from the observed data $Z^{(j)}, j \in \{1, \dots, p\}$.
 58 The ϵ_i 's are the residual differences between the output variable values and the RVFL model.

This type of model can be seen as a one explaining y_i , by finding a compromise between linear and potentially non-linear effects of the original predictors $Z^{(j)}$ and transformed predictors

$$\Phi(\mathbf{Z})^{(l)} = g \left(\sum_{j=1}^p W^{(j,l)} Z_i^{(j)} \right)$$

$\{1, \dots, L\}$ on the response. Common choices for function g in neural networks regression are the sigmoid activation function

$$g : x \mapsto \frac{1}{1 + e^{-x}}$$

the hyperbolic tangent function,

$$g : x \mapsto \tanh(x) = \frac{e^x - e^{-x}}{e^x + e^{-x}}$$

or the Rectified Linear Units, known as ReLU

$$g : x \mapsto \max(x, 0)$$

59 The main differences between the RVFL framework and a *classical* SLFN framework are:

- 60 • The inclusion of a linear dependence between the output variable and the predictors: the *direct*
 61 *link*, $\beta_0 + \sum_{j=1}^p \beta_j Z_i^{(j)}$
- 62 • The elements $W^{(j,l)}$ of the hidden layer are typically not trained, but randomly and uniformly
 63 chosen on a given interval. Different ranges for these elements of the hidden layer are tested in
 64 [Zhang and Suganthan \(2016\)](#).

Solving for the optimal parameters β_j 's and γ_l 's can be done by applying directly a least squares regression of y on the set of observed and transformed predictors. But since these input predictors are likely to be highly correlated - especially in our setting, with time series data - we do not search each of these parameters on the entire line, but in restricted regions where we have:

$$\sum_{j=1}^p \beta_j^2 \leq u$$

and

$$\sum_{l=1}^L \gamma_l^2 \leq v$$

65 for $u, v \in \mathbb{R}^*$. That is, applying some kind of Tikhonov regularization or ridge regression model (Hoerl
66 and Kennard (1970)) of y on the set of observed and transformed predictors. Having two constraints
67 instead of one, allows for more flexibility in the covariance structure between the predictors and the
68 output, with β_j 's and γ_l 's moving in separate balls. For these constraints to be applicable, the input
69 variables will need to be standardized, so as to be expressed on the same scales, and the response
70 variable will be centered.

71 Imposing these restrictions to the model's parameters increases their interpretability - by reducing
72 their variance -, at the expense of a slight increase in in-sample bias. It also prevents the model from
73 overfitting the data as in ridge regression (Hoerl and Kennard (1970)). One of the advantages of RVFL
74 networks is that they are relatively fast to train, due to the availability of closed-form formulas for the
75 model's parameters, as it will be presented in the next section.

76 On the other hand, RVFL networks incorporate some randomness in the hidden layer, which
77 makes each model relatively dependent on the choice of a simulation *seed*. Each *seed* would indeed
78 produce a different set of parameters β_j 's and γ_l 's for the model. For that reason, we will also use
79 sequences of deterministic quasi-random numbers in the hidden layer. The elements $W^{(j,l)}$ of the
80 hidden layer are taken from a quasi-random (deterministic) *sobol* sequence on $[0, 1]$, which is shifted in
81 such a way that they belong to $[-1, 1]$.

Sobol sequences are part of quasi-random numbers, which are also called *low discrepancy* sequences. As described intuitively in Boyle and Tan (1997), the discrepancy of a sequence of N points in a subcube $V \in [0, 1)^d$ is defined as:

$$\sup_{V \in [0,1)^d} \left| \frac{\text{number of points in } V}{N} - v(V) \right|$$

where $v(V)$ is the volume of V . It describes how well the points are dispersed within V . The idea is to have points which are more or less equidispersed in V . Joe and Kuo (2008) describe the generation of the i^{th} term, j^{th} component ($x_{i,j}$) of a Sobol sequence. The generation starts with obtaining the binary representation of i . That is, obtaining i as:

$$i = \sum_k i_k 2^k = (\dots i_3 i_2 i_1)_2$$

82 For example, $5 = 1 \times 2^2 + 0 \times 2^1 + 1 \times 2^0$ can be expressed as $(101)_2$ in binary representation.
83 Then, by using the sequence of bits describing i in base 2, we can obtain $x_{i,j}$ as:

$$x_{i,j} = i_1 v_{1,j} \oplus i_2 v_{2,j} \oplus \dots \quad (1)$$

84 Where \oplus is a bitwise exclusive-or operation, and the numbers $v_{i,j}$ are called the direction numbers,
85 defined for $k \geq 1$ as:

$$v_{k,j} = \frac{m_{k,j}}{2^k} = \frac{2a_{1,j}m_{k-1,j} \oplus 2^2a_{2,j}m_{k-2,j} \oplus \dots \oplus 2^{s_j-1}a_{s_j-1,j}m_{k-s_j+1,j} \oplus 2^{s_j}m_{k-s_j,j} \oplus m_{k-s_j,j}}{2^k} \quad (2)$$

86 A few details on equation 2:

- 87 • The bitwise exclusive-or operation \oplus applied to two integers p and $q \in \{0, 1\}$ returns 1 if and
88 only if one of the two (but not both) inputs is equal to 1. Otherwise, $p \oplus q$ is equal to 0.
- The second term of the equation relies on primitive polynomials of degree s_j , with coefficients $a_{i,j}$ taken in $\{0, 1\}$:

$$x^{s_j} + a_{1,j}x^{s_j-1} + a_{2,j}x^{s_j-2} + \dots + a_{s_j-1,j}x + 1 \quad (3)$$

- 89 • The terms $m_{k,j}$ are obtained recursively, with the initial values $m_{1,j}, m_{2,j}, \dots, m_{k-s_j,j}$ chosen freely,
90 under the condition that $m_{k,j}, 1 \leq k \leq s_j$ is odd and less than 2^k .

91 A more complete treatment of *low discrepancy* sequences can be found in [Niederreiter \(1992\)](#). And
 92 an example with $s_j = 3$, $a_{1,j} = 0$, $a_{2,j} = 1$ is given in [Joe and Kuo \(2008\)](#).

93 2.2. Applying RVFL networks to multivariate time series forecasting

94 We consider $p \in \mathbb{N}^*$ time series $(X_t^{(j)})_{t \geq 0}$, $j = 1, \dots, p$, observed at $n \in \mathbb{N}^*$ discrete dates. We are
 95 interested in obtaining simultaneous forecasts of the p time series at time $n + h$, $h \in \mathbb{N}^*$, by allowing
 96 each of the p variables to be influenced by the others (in the spirit of VAR models, see [Lütkepohl](#)
 97 [\(2005\)](#)).

98 For this purpose, we use $k < n$ lags of each of the observed p time series. The output variables to
 99 be explained are:

$$Y^{(j)} = \left(X_n^{(j)}, \dots, X_{k+1}^{(j)} \right)^T \quad (4)$$

for $j \in \{1, \dots, p\}$. Where $X_n^{(j)}$ is the most contemporaneous observed value of the j^{th} time series,
 and $X_{k+1}^{(j)}$ was observed k dates earlier in time for $(X_t^{(j)})_{t \geq 0}$. These output variables are stored in a
 matrix:

$$\mathbf{Y} \in \mathbb{R}^{(n-k) \times p}$$

and the predictors are stored in a matrix:

$$\mathbf{X} \in \mathbb{R}^{(n-k) \times (k \times p)}$$

100 where \mathbf{X} consists in p blocks of k lags, for each one of the observed p time series. For example, the j_0^{th}
 101 block of \mathbf{X} , for $j_0 \in \{1, \dots, p\}$ contains in columns:

$$\left(X_{n-i}^{(j_0)}, \dots, X_{k+1-i}^{(j_0)} \right)^T \quad (5)$$

102 with $i \in \{1, \dots, k\}$. It is also possible to add other regressors, such as dummy variables, indicators
 103 of special events, but for clarity, we consider only the inclusion of lags.

As described in the previous section, an additional layer of transformed predictors is added to
 \mathbf{X} , in order to capture the potentially non-linear interactions between the predictors and the output
 variable. Adding the transformed predictors to the original ones, leads to a new matrix of predictors
 with dimensions $(n - k) \times (k \times p + L)$, where L is the number of nodes in the hidden layer. We are
 then looking for simultaneous predictions

$$\hat{X}_{n+h|n,\dots,1}^{(j)} =: \hat{X}_{n+h}^{(j)}$$

104 for $h \in \mathbb{N}^*$, and $j \in \{1, \dots, p\}$. This, is a *multi-task learning* problem (see [Caruana \(1998\)](#)), in which the
 105 output variables will all share the same set of predictors.

For example, we have $p = 2$ time series $(X_{t_1}^{(1)}, \dots, X_{t_5}^{(1)})$ and $(X_{t_1}^{(2)}, \dots, X_{t_5}^{(2)})$ observed at $n = 5$
 dates $t_1 < \dots < t_5$, with $k = 2$ lags, and $L = 3$ nodes in the hidden layer. In this case, the response
 variables are stored in:

$$\mathbf{Y} = \begin{pmatrix} X_{t_5}^{(1)} & X_{t_5}^{(2)} \\ X_{t_4}^{(1)} & X_{t_4}^{(2)} \\ X_{t_3}^{(1)} & X_{t_3}^{(2)} \end{pmatrix}$$

The predictors are stored in:

$$\mathbf{X} = \begin{pmatrix} X_{t_4}^{(1)} & X_{t_3}^{(1)} & X_{t_4}^{(2)} & X_{t_3}^{(2)} \\ X_{t_3}^{(1)} & X_{t_2}^{(1)} & X_{t_3}^{(2)} & X_{t_2}^{(2)} \\ X_{t_2}^{(1)} & X_{t_1}^{(1)} & X_{t_2}^{(2)} & X_{t_1}^{(2)} \end{pmatrix}$$

And the coefficients in the hidden layer are:

$$\mathbf{W} = \begin{pmatrix} W^{(1,1)} & W^{(1,2)} & W^{(1,3)} \\ W^{(2,1)} & W^{(2,2)} & W^{(2,3)} \\ W^{(3,1)} & W^{(3,2)} & W^{(3,3)} \\ W^{(4,1)} & W^{(4,2)} & W^{(4,3)} \end{pmatrix}$$

106 2.3. Solving for $\hat{\beta}$'s and $\hat{\gamma}$'s

We let y be the j_0^{th} column (out of p) of the response matrix \mathbf{Y} , and $\Phi(\mathbf{X})$ be the matrix of transformed predictors obtained from \mathbf{X} by the hidden layer described at the beginning of section 2.1. We also denote the set of regression parameters associated with this j_0^{th} time series, as:

$$\beta_m^{(j_0)} =: \beta_m$$

and

$$\gamma_l^{(j_0)} =: \gamma_l$$

for $m \in \{1, \dots, k\}; l \in \{1, \dots, L\}$. Solving for the regression parameters for the j_0^{th} time series, under the constraints

$$\sum_{m=1}^{k \times p} \beta_m^2 \leq u$$

and

$$\sum_{l=1}^L \gamma_l^2 \leq v$$

for $u, v \in \mathbb{R}^*$, leads to minimizing a penalized residual sum of squares. Hence, for vectors $\beta \in \mathbb{R}^{(k \times p)}$ and $\gamma \in \mathbb{R}^L$ containing the regression parameters, we obtain the Lagrangian:

$$\mathcal{L}(\mathbf{X}; \beta, \gamma) = (y - \mathbf{X}\beta - \Phi(\mathbf{X})\gamma)^T (y - \mathbf{X}\beta - \Phi(\mathbf{X})\gamma) + \lambda_1 \beta^T \beta + \lambda_2 \gamma^T \gamma$$

107 where λ_1 and λ_2 are Lagrange multipliers. Taking the first derivatives of \mathcal{L} relative to β and γ
108 leads to:

$$\begin{aligned} \frac{\partial \mathcal{L}(\mathbf{X}; \beta, \gamma)}{\partial \beta} &= -y^T \mathbf{X} - \mathbf{X}^T y + 2(\mathbf{X}^T \mathbf{X})\beta + \mathbf{X}^T \Phi(\mathbf{X})\gamma + (\Phi(\mathbf{X})\gamma)^T \mathbf{X} + 2\lambda_1 \beta \\ &= 2(\mathbf{X}^T \mathbf{X} + \lambda_1 I_{k \times p})\beta - y^T \mathbf{X} - \mathbf{X}^T y + \mathbf{X}^T \Phi(\mathbf{X})\gamma + (\Phi(\mathbf{X})\gamma)^T \mathbf{X} \\ &= 2(\mathbf{X}^T \mathbf{X} + \lambda_1 I_{k \times p})\beta - 2\mathbf{X}^T y + 2\mathbf{X}^T \Phi(\mathbf{X})\gamma \end{aligned}$$

109 where $I_{k \times p}$ is the identity matrix with dimensions $(k \times p) \times (k \times p)$ and equivalently

$$\frac{\partial \mathcal{L}(\mathbf{X}; \beta, \gamma)}{\partial \gamma} = 2(\Phi(\mathbf{X})^T \Phi(\mathbf{X}) + \lambda_2 I_L)\gamma - 2\Phi(\mathbf{X})^T y + 2\Phi(\mathbf{X})^T \mathbf{X}\beta$$

where I_L is the identity matrix with dimensions $L \times L$. And setting these first derivatives to 0 leads to:

$$\begin{cases} (\mathbf{X}^T \mathbf{X} + \lambda_1 I_{k \times p})\beta + \mathbf{X}^T \Phi(\mathbf{X})\gamma = \mathbf{X}^T y \\ (\Phi(\mathbf{X})^T \Phi(\mathbf{X}) + \lambda_2 I_L)\gamma + \Phi(\mathbf{X})^T \mathbf{X}\beta = \Phi(\mathbf{X})^T y \end{cases}$$

That is:

$$\begin{pmatrix} \mathbf{X}^T\mathbf{X} + \lambda_1 I_{k \times p} & \mathbf{X}^T\Phi(\mathbf{X}) \\ \Phi(\mathbf{X})^T\mathbf{X} & \Phi(\mathbf{X})^T\Phi(\mathbf{X}) + \lambda_2 I_L \end{pmatrix} \begin{pmatrix} \beta \\ \gamma \end{pmatrix} = \begin{pmatrix} \mathbf{X}^T\mathbf{y} \\ \Phi(\mathbf{X})^T\mathbf{y} \end{pmatrix}$$

110 Now, if we denote:

$$A = \begin{pmatrix} \mathbf{X}^T\mathbf{X} + \lambda_1 I_{k \times p} & \mathbf{X}^T\Phi(\mathbf{X}) \\ \Phi(\mathbf{X})^T\mathbf{X} & \Phi(\mathbf{X})^T\Phi(\mathbf{X}) + \lambda_2 I_L \end{pmatrix} =: \begin{pmatrix} B & C^T \\ C & D \end{pmatrix}$$

and $S = D - CB^+C^T$. Then, using the algorithm described in [Cormen \(2009\)](#) for blockwise matrix inversion, we obtain:

$$A^+ = \begin{pmatrix} B^+ + B^+C^T S^+ C B^+ & -B^+C^T S^+ \\ -S^+ C B^+ & S^+ \end{pmatrix} =: \begin{pmatrix} A_1^+ & A_2^+ \\ A_3^+ & A_4^+ \end{pmatrix}$$

111 where S^+ and B^+ are the Moore-Penrose pseudo-inverse ([Penrose \(1955\)](#)) of matrixes S and B .
112 Hence for each column y of \mathbf{Y} , we have the solutions:

$$\begin{pmatrix} \hat{\beta} \\ \hat{\gamma} \end{pmatrix} = \begin{pmatrix} A_1^+ & A_2^+ \\ A_3^+ & A_4^+ \end{pmatrix} \begin{pmatrix} \mathbf{X}^T y \\ \Phi(\mathbf{X})^T y \end{pmatrix}$$

113 And the whole set of parameters, for all the p observed time series is given by:

$$\begin{pmatrix} \underline{\hat{\beta}} \\ \underline{\hat{\gamma}} \end{pmatrix} := \begin{pmatrix} A_1^+ & A_2^+ \\ A_3^+ & A_4^+ \end{pmatrix} \begin{pmatrix} \mathbf{X}^T \mathbf{Y} \\ \Phi(\mathbf{X})^T \mathbf{Y} \end{pmatrix}$$

114 The objective function to be minimized (the least squares) is convex, and so is the set of feasible
115 solutions. The solutions $\underline{\hat{\beta}}$ and $\underline{\hat{\gamma}}$ found here, are hence global minima.

116 2.4. h -steps ahead forecasts and use of dynamic regression

117 Having obtained the optimal set of parameters $\underline{\hat{\beta}}$ and $\underline{\hat{\gamma}}$ as described in the previous section, a new
118 set of predictors is constructed by using the former output variables contained in response matrix \mathbf{Y} 's
119 columns. The first k elements of each one of the p columns of \mathbf{Y} , which are the most contemporaneous
120 values of the p series, constitute the new predictors.

121 Hence, if we denote the new predictors as:

$$\mathbf{X}_n^* = \left(X_n^{(1)}, \dots, X_{n-k+1}^{(1)}, \dots, X_n^{(p)}, \dots, X_{n-k+1}^{(p)} \right) \quad (6)$$

122 The 1-step ahead forecasts are obtained as:

$$\left(\hat{X}_{n+1}^{(1)}, \dots, \hat{X}_{n+1}^{(p)} \right) = \left(\mathbf{X}_n^* \quad \Phi(\mathbf{X}_n^*) \right) \begin{pmatrix} \underline{\hat{\beta}} \\ \underline{\hat{\gamma}} \end{pmatrix}$$

123 The h -step ahead forecasts are obtained in a similar fashion; with the new forecasts
124 $\left(\hat{X}_{n+1}^{(1)}, \dots, \hat{X}_{n+1}^{(p)} \right)$ being added to the set of most contemporaneous values of the p series, and used as
125 part of the new predictors.

126 In order to obtain confidence intervals around the point forecasts, we fit an ARIMA model to the
127 in-sample residuals ϵ_i of each one of the p time series, as in dynamic regression models (see [Pankratz \(2012\)](#)). An illustration can be found in the next section. Other models for the autocorrelated residuals
128 could be envisaged, though.
129

130 3. Numerical examples

131 3.1. A Dynamic Nelson-Siegel example

132 The following examples are not exhaustive benchmarks, but aim at illustrating the forecasting
133 capabilities of the model described in this paper. All the results on RVFL use the ReLU activation
134 function. We use calibrated discount rates data from [Deutsche Bundesbank website](#), observed on
135 a monthly basis, from the beginning of 2002 to the end 2015. There are 167 curves, observed at 50
136 maturities in the dataset. We obtain curves' forecasts in a Dynamic Nelson Siegel [Nelson and Siegel](#)
137 (1987) framework (DNS), in the spirit of [Diebold and Li \(2006\)](#) and other similar models ¹.

138 In figure 2, we present the data that we use, and table 1 contains a summary of these data;
139 the minimum, maximum, median, first and third quartiles of the discount rates observed at given
140 maturities. There are alternate cycles of increases and decreases of the discount rates, with generally
141 a decreasing trend. Some of the discount rates, at the most recent dates, and lower maturities, are
142 negative.

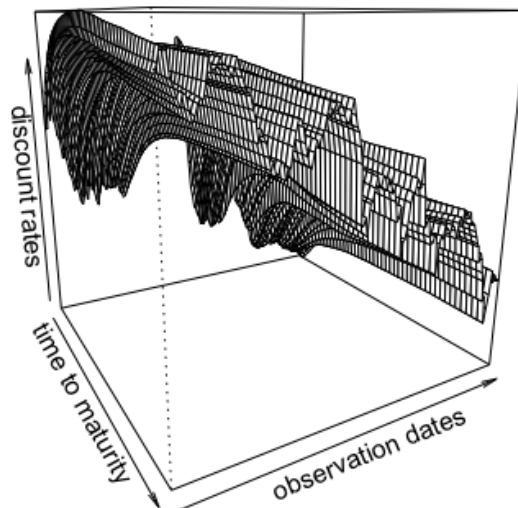


Figure 2. Observed discount rates from Deutsche Bundesbank website, from 2002 to the end 2015

¹ [Diebold and Rudebusch \(2013\)](#): "there are by now literally hundreds of DNS applications involving model fitting and forecasting"

Table 1. Summary of observed discount rates from Deutsche Bundesbank website, from 2002 to the end 2015

Maturity	Min	1st Qrt	Median	3rd Qrt	Max
1	-0.116	0.858	2.045	3.072	5.356
5	0.170	1.327	2.863	3.807	5.146
15	0.711	2.616	3.954	4.702	5.758
30	0.805	2.594	3.962	4.814	5.784
50	0.749	2.647	3.630	4.590	5.467

In the DNS framework, the spot interest rates observed at time t , for time to maturity τ are modeled as:

$$R_t(\tau) = \alpha_{1,t} + \alpha_{2,t} \left(\frac{1 - e^{-\tau/\lambda}}{e^{-\tau/\lambda}} \right) + \alpha_{3,t} \left(\frac{1 - e^{-\tau/\lambda}}{e^{-\tau/\lambda}} - e^{-\tau/\lambda} \right) \quad (7)$$

143 The factor loadings $1, \left(\frac{1 - e^{-T/\lambda}}{e^{-T/\lambda}} \right)$ and $\left(\frac{1 - e^{-T/\lambda}}{e^{-T/\lambda}} - e^{-T/\lambda} \right)$ are used to represent the level, slope,
 144 and curvature of the Yield Curve. We obtain estimations of $\alpha_{i,t}, i = 1, \dots, 3$ for each cross-section of
 145 yields by fixing λ , and doing a least squares regression on the factor loadings. The three time series
 146 $\alpha_{i,t}, i = 1, \dots, 3$ associated to the loadings for each cross-section of yields, are those that we wish to
 147 forecast simultaneously, by using an RVFL model.

148 This type of model (DNS) cannot be used for no-arbitrage pricing as is, but it could be useful for
 149 example, for *stressing* the yield curve factors under the historical probability. It can however be made
 150 arbitrage-free, if necessary (see [Diebold and Rudebusch \(2013\)](#)). We will benchmark the RVFL model
 151 applied to the three time series $\alpha_{i,t}, i = 1, \dots, 3$, against ARIMA and VAR models. [Diebold and Li](#)
 152 [\(2006\)](#) applied an autoregressive AR(1) model separately to each one of the parameters, $\alpha_{i,t}, i = 1, \dots, 3$.

153 We will apply to these parameters' series: an ARIMA model ([Hyndman and Khandakar \(2008\)](#)),
 154 and a Vector Autoregressive model (VAR, see [Pfaff et al. \(2008\)](#) and [Lütkepohl \(2005\)](#)); with the
 155 parameter λ of the DNS factor loadings, used as an *hyperparameter* for the time series cross-validation.
 156 In the RVFL and the VAR model, the number of lags is also used as an *hyperparameter* for the
 157 cross-validation. For the RVFL, the most recent values of $\alpha_{i,t}, i = 1, \dots, 3$ are stored in matrix \mathbf{Y} ,
 158 as described in section 2.3, ordered by *date of arrival*, whereas matrix \mathbf{X} contains the lags of the three
 159 series.

160 A rolling forecasting methodology (see [Bergmeir et al. \(2015\)](#)) is implemented in order to obtain
 161 these benchmarks. A fixed 12 months-length window for training the model, and the following 12
 162 months for testing, the origin of the training set is then advanced of 1 month, and the training/testing
 163 procedure is repeated. The measure of forecasting performance is the Root Mean Squared Error
 164 (*RMSE*).

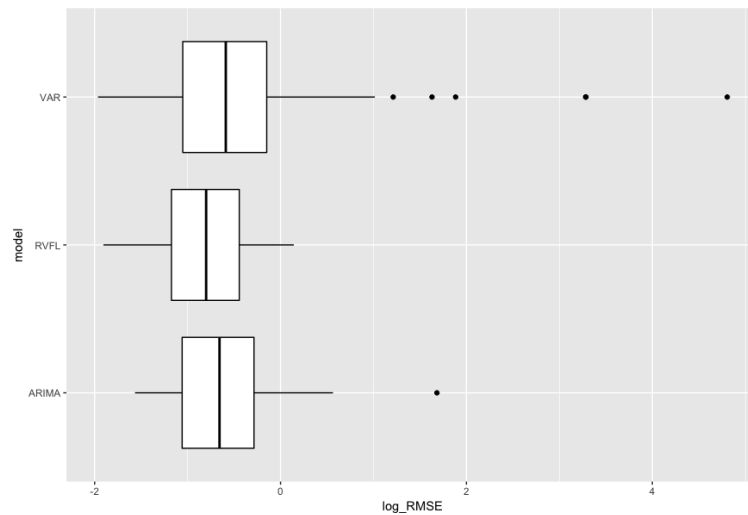


Figure 3. Distribution of out-of-sample $\log(RMSE)$, for ARIMA, VAR, and RVFL

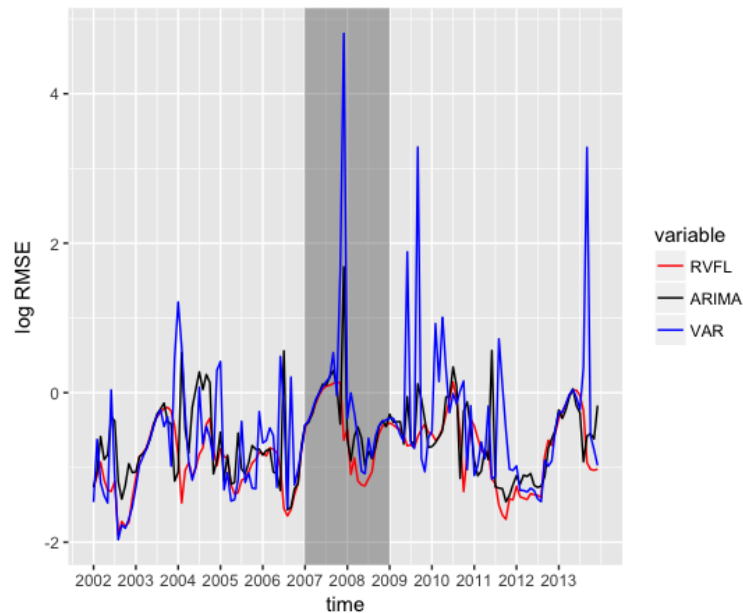


Figure 4. Out-of-sample $\log(RMSE)$, for ARIMA, VAR, and RVFL over time

165 Figure 3 presents boxplots for the distribution of out-of-sample errors obtained in the
 166 cross-validation procedure, and figure 4 presents the 12 months-ahead out-of-sample errors over
 167 time. ARIMA (separate (Hyndman and Khandakar (2008)) ARIMA models applied to each series
 168 $\alpha_{i,t}, i = 1, \dots, 3$) gives good results, as already suggested by Diebold and Li (2006). They are nearly
 169 comparable to results from RVFL, but a bit more volatile, with an outlier point observed on the
 170 $\log(RMSE)$ box plot.

171 The unrestricted VAR model results include more volatility than the two other methods on this
 172 specific example, especially in the period of financial crisis going from 2007 to 2009, as seen on figure 4.
 173 Table 2 is to be read in conjunction with the $\log(RMSE)$ box plot presented in figure 3. It summarises
 174 the results obtained by the different methods on the out-of-sample $RMSE$. Table 3 contains 95%
 175 confidence intervals around the mean of the differences between the three methods.

Table 2. Comparison of 12 months ahead out-of-sample *RMSE*, for the ARIMA, RVFL, and VAR

Method	Min	1st Qrt	Median	Mean	3rd Qrt	Max
RVFL	0.1487	0.3092	0.4491	0.5041	0.6414	1.1535
ARIMA	0.2089	0.3470	0.5187	0.6358	0.7516	5.3798
VAR	0.1402	0.3493	0.5549	1.9522	0.8619	122.2214

Table 3. 95% confidence interval around the difference of out-of-sample *RMSE*

Method	Lower bound	Upper bound	Mean
RVFL - ARIMA	-0.2116	-0.0518	-0.1317
RVFL - VAR	-3.1888	0.2927	-1.4480
ARIMA - VAR	-2.9937	0.3610	-1.3163

176 Another advantage of RVFL over ARIMA or AR(1) in this context is that, it would be possible
 177 to add other variables to the RVFL regression, such as inflation, or dummy variables for external
 178 events, and combine their effects. It is also possible to stress one variable, and see the effects on the
 179 other variables, as presented in the appendix section 5.1: the parameter $\alpha_{1,t}$ is increased (from 0.75 to
 180 1.25) and decreased (from 0.75 to 0.25), and the other parameters $\alpha_{2,t}$ and $\alpha_{3,t}$ forecasts move slightly,
 181 consecutively to these *stresses*. The corresponding median forecast curves for these stresses, and some
 182 additional ones, are presented in figure 5.

183 3.2. Forecasting 1 year, 10 years and 20 years spot rates

184 For this second example, we forecast the 1-year, 10-years and 20-years spot rates time series from
 185 the previous dataset, on a 12-months horizon. As described in the previous section, we use a rolling
 186 forecasting methodology, with a training window of 12 months length.

187 Figure 6 presents the three time series of data, and a summary of the data can be found in tables 4
 188 and 5.

Table 4. Summary of the data for 1 year, 10 years and 20 years spot rates time series (in %)

Method	Min	1st Qrt	Median	Mean	3rd Qrt	Max
1y rate	-0.116	0.858	2.045	2.062	3.072	5.356
10y rate	0.560	2.221	3.581	3.322	4.354	5.570
20y rate	0.790	2.685	4.050	3.782	4.830	5.850

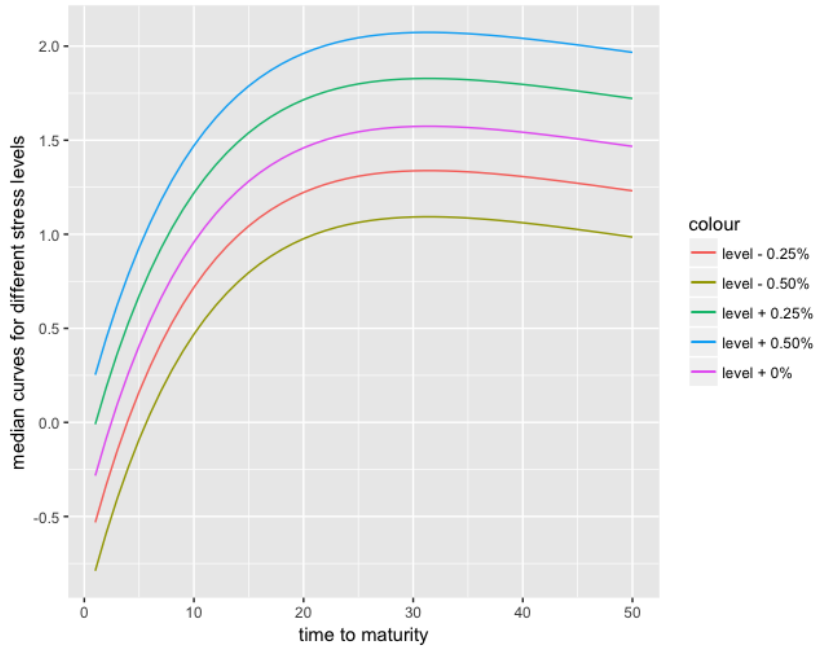


Figure 5. 12 months-ahead median curves, for stressed yield curve level $\alpha_{1,t}$

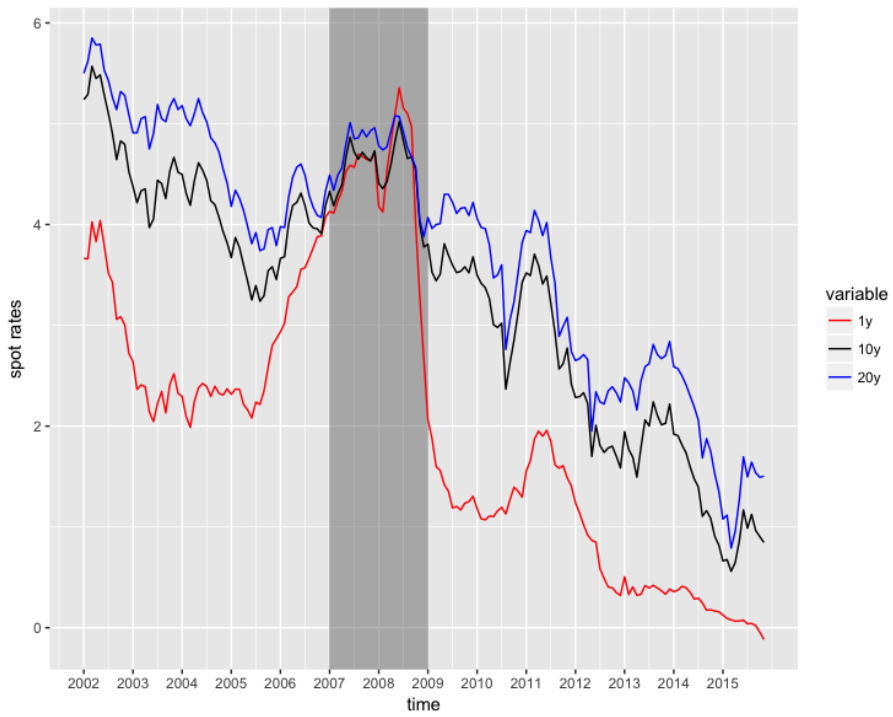


Figure 6. 1-year, 10-years and 20-years spot rates time series data

Table 5. Summary of data for 1 year, 10 years and 20 years spot rates time series

Correlations	1y rate	10y rate	20y rate
1y rate	1.0000	0.8729	0.8118
10y rate	0.8729	1.0000	0.9900
20y rate	0.8118	0.9900	1.0000

189 The three time series globally exhibit a decreasing trend, and are highly positively correlated. The
 190 spot rates for short-term maturities can also be negative, as it has been observed recently in 2016. The
 191 spreads between the spot rates time series are extremely narrow during the 2007-2009 crisis. The tables
 192 below contain the results of a comparison between the RVFL model and an unrestricted VAR model
 193 (with one lag, *best* parameter found) on the forecasting problem. The *best* RVFL model, with the lowest
 194 out-of-sample *RMSE*, uses one lag, four hidden nodes, and $\lambda_1 = 5.80$, $\lambda_2 = 19.66$.

Table 6. Comparison of 12 months ahead out-of-sample *RMSE*, for the RVFL, and VAR

Method	Min	1st Qrt	Median	Mean	3rd Qrt	Max
RVFL	0.1675	0.2906	0.4704	0.5452	0.6469	1.8410
VAR	0.1382	0.4025	0.6469	1.0310	1.0750	13.020

Table 7. 95% confidence interval around the difference of out-of-sample *RMSE*

Method	Lower bound	Upper bound	Mean
RVFL-VAR	-0.2622	-0.7087	-0.4854

195 3.3. Forecasting on a longer horizon, with a longer training window

196 In this third example, as in section 3.1, we apply the DNS framework to the forecasting of spot
 197 rates. But with a longer training set (36 months), and a longer horizon for the test set (36 months as
 198 well). We use interest rate swaps data from the Federal Reserve Bank of St Louis website², observed
 199 on a monthly basis from July 2000 to September 2016, with maturities equal to 1, 2, 3, 4, 5, 7, 10, 30, and
 200 a tenor equal to three months.

201 On figure 7, we present three of the eight time series of swap rates, observed for time to maturities
 202 equal to 3, 10 and 30. The swap rates for different maturities generally exhibit a decreasing trend, and
 203 are nearly equal to 0 by the end of 2016, for the shortest maturities.

204 We also observe that the spreads between swap rates with different maturities start to narrow in
 205 2006 until the end of 2007, and the swap rates for short term maturities are relatively high during the
 206 same period. This is the period corresponding to the Liquidity and Credit Crunch 2007-2008. Table 8
 207 presents the descriptive statistics for these three time series.

208 All the swap rates (for all the maturities available) were then transformed into zero rates, by
 209 using a single curve calibration methodology (that is, ignoring the counterparty credit risk) with
 210 linear interpolation between the swaps' maturities. Then, the Nelson & Siegel model was used for
 211 fitting and forecasting the curves in a DNS framework, with both `auto.arima` and the RVFL model

² Available at <https://fred.stlouisfed.org/categories/32299>

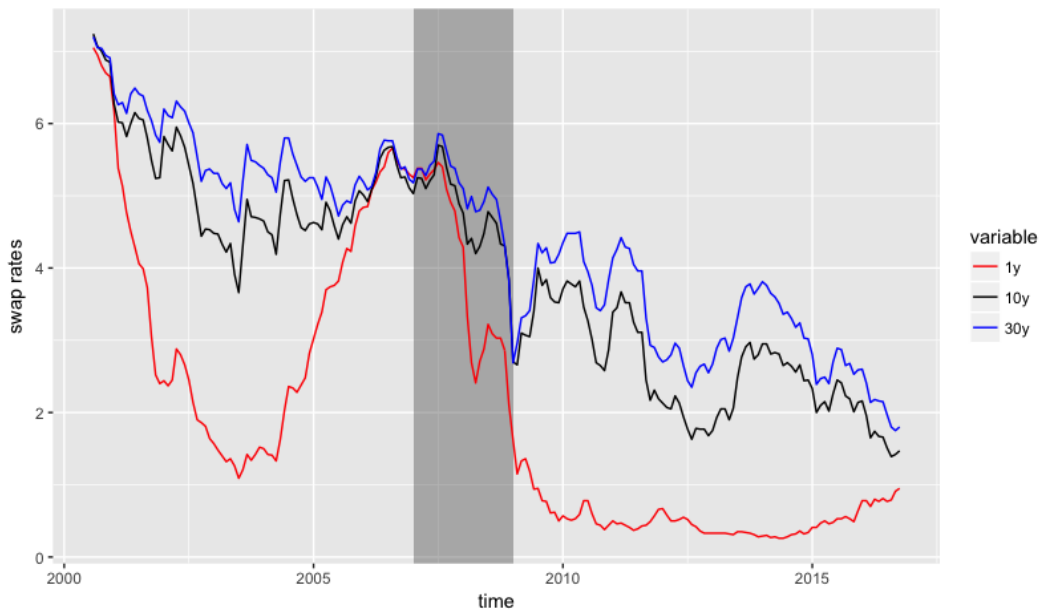


Figure 7. Swap rates data (in %) from St Louis Federal Reserve Bank, at maturities 1, 10, 30

Table 8. Descriptive statistics of St Louis Federal Reserve data for 1y, 10y and 30y swap rates (in %)

Maturity	Min.	1st Qrt	Median	Mean	3rd Qrt	Max.
1	0.260	0.500	1.340	2.108	3.360	7.050
10	1.390	2.610	4.190	3.881	5.020	7.240
30	1.750	3.270	4.650	4.404	5.375	7.200

212 presented in this paper, applied to the three factors. In the fashion of section 3.1. But now, we obtain
 213 36-months ahead forecasts, from a rolling training windows with a fixed 36 months length. The
 214 average out-of-sample *RMSE* are then calculated for each method.

215 The *best* hyperparameters - associated with the lowest out-of-sample average *RMSE* - for each
 216 model are obtained through a search on a grid of values. We have:

- 217 • DNS with ARIMA (`auto.arima`): $\lambda = 1.4271$ (Nelson Siegel parameter)
- 218 • DNS with RVFL: **number of lags** for each series: 1, **activation function**: ReLU, **number of nodes**
 219 in the hidden layer: 45, $\lambda_1 = 4.6416$, $\lambda_2 = 774.2637$ (RVFL parameters) and $\lambda = 24$ (Nelson
 220 Siegel parameter)

221 With these parameters, the results detailed in table 9 are obtained, for the out-of-sample *RMSE*.
 222 A 95% confidence interval around the difference of out-of-sample *RMSE* between ARIMA (applied to
 223 each one of the three factors) and RVFL is presented in table 10.

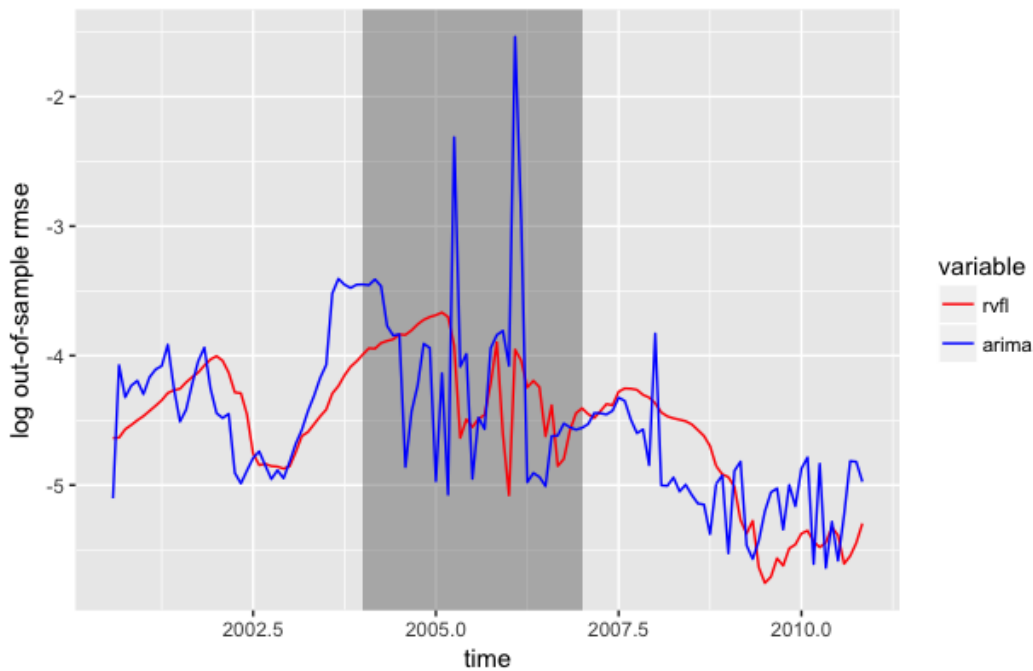
Table 9. Descriptive statistics for out-of-sample *RMSE*, with rolling training window = 36 months, and testing window = 36 months

Method	Min.	1st Qrt	Median	Mean	3rd Qrt	Max.	Std. Dev
ARIMA	0.0036	0.0070	0.0104	0.0149	0.0161	0.2150	0.0213
RVFL	0.0032	0.0078	0.0115	0.0120	0.0148	0.0256	0.0055

Table 10. 95% confidence interval around the difference of out-of-sample $RMSE$

Method	Lower bound	Upper bound	Mean
RVFL-ARIMA	-0.0064	0.0007	-0.0028

224 Figure 8 presents the evolution of the out-of-sample $\log(RMSE)$ over the training/testing
 225 windows. The grey rectangle indicating the Liquidity and Credit crunch is larger here, because
 226 in this example, a training set starting in 2004 has its test set starting 36 months later, in 2007. Again,
 227 we observe that the results from the RVFL model exhibit a low out-of-sample error, along with a low
 228 volatility.

**Figure 8.** Out-of-sample $\log(RMSE)$, for ARIMA and RVFL over time

229 Figure 9, presents the convergence of the out-of-sample $\log(RMSE)$ for the DNS + RVFL model
 230 from this section, as a function of $\log(\lambda_1)$ and $\log(\lambda_2)$. λ_1 and λ_2 both range from 10^{-2} to 10^4 , with ten
 231 equally-spaced points each (hence, a grid of one hundred points $(\log(\lambda_1), \log(\lambda_2), \log(RMSE))$).

232 The number of nodes in the hidden layer is equal to 45, and the value of λ , parameter from the
 233 Nelson and Siegel (1987) model presented in section 3.1, is fixed and equal to 24. The one hundred
 234 points $(\log(\lambda_1), \log(\lambda_2), \log(RMSE))$ that we use for figure 9 can be found in appendix .3.

235 There is a rectangular region at the top, in the middle of the figure, where the $\log(RMSE)$ is the
 236 lowest. In this region, the lowest value of the out-of-sample $\log(RMSE)$ is observed for $\lambda_1 = 4.6416$
 237 and $\lambda_2 = 464.1589$ and the out-of-sample $RMSE$ is equal to 0.01206 (75th point in appendix .3).

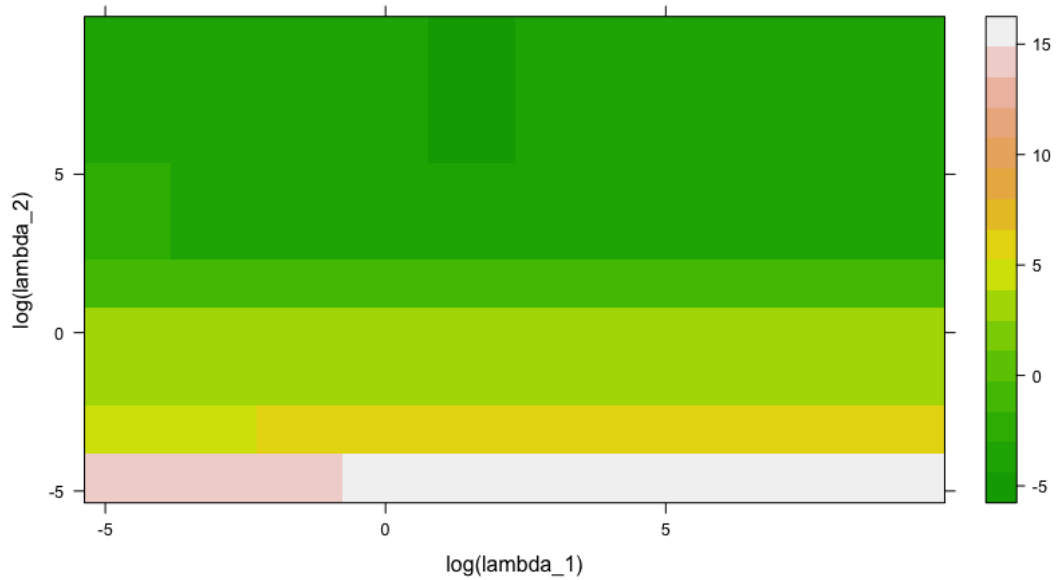


Figure 9. Out-of-sample $\log(RMSE)$, as a function of λ_1 and λ_2

238 4. Conclusion

239 We present a model which could be used for multiple time series forecasting, based on a single
 240 layer quasi-randomized neural network. In this model, the lags of the different time series are used
 241 as in a dynamic regression model, and include the response variable lags. An additional layer of
 242 variables is added to the regression, whose nodes are not trained but obtained from a low discrepancy
 243 sequence. It is possible to add new variables to the regression, as indicators of special events, or to
 244 stress one variable, and observe the implied effect on the others' forecast. The model is tested on raw
 245 historical spot rates, and in a Dynamic Nelson Siegel framework. It produces *robust* forecast results
 246 when compared to other usual (unpenalized) models in the same framework.

247 **5. Appendix**248 *5.1. Mean forecast and confidence intervals for $\alpha_{i,t}, i = 1, \dots, 3$ forecasts*249 $\alpha_{1,t}$:

250	alpha1	y_lo80	y_hi80	y_lo95	y_hi95
251	13	0.7432724	0.6852024	0.8013425	0.6544620
252	14	0.7357374	0.6776673	0.7938074	0.6469269
253	15	0.7378042	0.6797342	0.7958742	0.6489938
254	16	0.7408417	0.6827717	0.7989118	0.6520313
255	17	0.7407904	0.6827204	0.7988604	0.6519800
256	18	0.7404501	0.6823801	0.7985201	0.6516396
257	19	0.7403603	0.6822903	0.7984303	0.6515498
258	20	0.7403981	0.6823281	0.7984681	0.6515876
259	21	0.7404788	0.6824087	0.7985488	0.6516683
260	22	0.7404786	0.6824086	0.7985487	0.6516682
261	23	0.7404791	0.6824091	0.7985491	0.6516686
262	24	0.7404758	0.6824058	0.7985458	0.6516654

263 $\alpha_{2,t}$:

264	alpha2	y_lo80	y_hi80	y_lo95	y_hi95
265	13	-1.250640	-1.351785	-1.149495	-1.405328
266	14	-1.243294	-1.344439	-1.142149	-1.397982
267	15	-1.241429	-1.342574	-1.140284	-1.396117
268	16	-1.243868	-1.345014	-1.142723	-1.398557
269	17	-1.244483	-1.345628	-1.143338	-1.399171
270	18	-1.241865	-1.343010	-1.140719	-1.396553
271	19	-1.240814	-1.341959	-1.139669	-1.395502
272	20	-1.240371	-1.341516	-1.139226	-1.395059
273	21	-1.240237	-1.341382	-1.139092	-1.394925
274	22	-1.240276	-1.341421	-1.139131	-1.394964
275	23	-1.240329	-1.341474	-1.139184	-1.395017
276	24	-1.240308	-1.341453	-1.139163	-1.394996

277 $\alpha_{3,t}$:

278	alpha3	y_lo80	y_hi80	y_lo95	y_hi95
279	13	4.584836	4.328843	4.757406	4.215410
280	14	4.546167	4.307253	4.849862	4.163634
281	15	4.527651	4.201991	4.803004	4.042913
282	16	4.513810	4.216525	4.850160	4.048812
283	17	4.517643	4.176214	4.828735	4.003502
284	18	4.523109	4.203064	4.866713	4.027406
285	19	4.522772	4.178489	4.848760	4.001079
286	20	4.521846	4.191833	4.866066	4.013374
287	21	4.521382	4.177560	4.854171	3.998472
288	22	4.521451	4.186714	4.864755	4.007248
289	23	4.521772	4.178995	4.857897	3.999300
290	24	4.521862	4.184734	4.864155	4.004903

291 5.2. Stressed forecast ($\alpha_{1,t} + 0.5\%$) and confidence intervals for $\alpha_{i,t}, i = 1, \dots, 3$ forecasts292 $\alpha_{1,t}$:

293	alpha1	y_lo80	y_hi80	y_lo95	y_hi95	
294	13	1.25	1.19193	1.30807	1.16119	1.33881
295	14	1.25	1.19193	1.30807	1.16119	1.33881
296	15	1.25	1.19193	1.30807	1.16119	1.33881
297	16	1.25	1.19193	1.30807	1.16119	1.33881
298	17	1.25	1.19193	1.30807	1.16119	1.33881
299	18	1.25	1.19193	1.30807	1.16119	1.33881
300	19	1.25	1.19193	1.30807	1.16119	1.33881
301	20	1.25	1.19193	1.30807	1.16119	1.33881
302	21	1.25	1.19193	1.30807	1.16119	1.33881
303	22	1.25	1.19193	1.30807	1.16119	1.33881
304	23	1.25	1.19193	1.30807	1.16119	1.33881
305	24	1.25	1.19193	1.30807	1.16119	1.33881

306 $\alpha_{2,t}$:

307	alpha2	y_lo80	y_hi80	y_lo95	y_hi95	
308	13	-1.222568	-1.323713	-1.121423	-1.377256	-1.067880
309	14	-1.219401	-1.320546	-1.118256	-1.374089	-1.064713
310	15	-1.211361	-1.312506	-1.110216	-1.366049	-1.056673
311	16	-1.216213	-1.317358	-1.115068	-1.370901	-1.061525
312	17	-1.215266	-1.316411	-1.114121	-1.369954	-1.060578
313	18	-1.211474	-1.312619	-1.110329	-1.366162	-1.056786
314	19	-1.210329	-1.311474	-1.109183	-1.365017	-1.055640
315	20	-1.209610	-1.310755	-1.108465	-1.364298	-1.054922
316	21	-1.209648	-1.310793	-1.108503	-1.364336	-1.054960
317	22	-1.209601	-1.310746	-1.108456	-1.364289	-1.054913
318	23	-1.209688	-1.310833	-1.108542	-1.364376	-1.055000
319	24	-1.209653	-1.310798	-1.108508	-1.364341	-1.054965

320 $\alpha_{3,t}$:

321	alpha3	y_lo80	y_hi80	y_lo95	y_hi95	
322	13	4.500390	4.244398	4.672961	4.130964	4.786394
323	14	4.482948	4.244035	4.786643	4.100415	4.930263
324	15	4.441841	4.116182	4.717194	3.957103	4.876272
325	16	4.441744	4.144459	4.778094	3.976746	4.945808
326	17	4.439609	4.098181	4.750701	3.925469	4.923413
327	18	4.447151	4.127105	4.790755	3.951448	4.966412
328	19	4.446164	4.101881	4.772152	3.924471	4.949562
329	20	4.445421	4.115407	4.789641	3.936949	4.968099
330	21	4.445411	4.101589	4.778200	3.922501	4.957289
331	22	4.445491	4.110754	4.788795	3.931287	4.968262
332	23	4.445937	4.103160	4.782062	3.923465	4.961756
333	24	4.446012	4.108885	4.788306	3.929053	4.968137

334 *Appendix .1 Mean forecast and confidence intervals for $\alpha_{i,t}$, $i = 1, \dots, 3$ forecasts*335 $\alpha_{1,t}$:

336	alpha1	y_lo80	y_hi80	y_lo95	y_hi95	
337	13	0.7432724	0.6852024	0.8013425	0.6544620	0.8320829
338	14	0.7357374	0.6776673	0.7938074	0.6469269	0.8245478
339	15	0.7378042	0.6797342	0.7958742	0.6489938	0.8266147
340	16	0.7408417	0.6827717	0.7989118	0.6520313	0.8296522
341	17	0.7407904	0.6827204	0.7988604	0.6519800	0.8296009
342	18	0.7404501	0.6823801	0.7985201	0.6516396	0.8292605
343	19	0.7403603	0.6822903	0.7984303	0.6515498	0.8291707
344	20	0.7403981	0.6823281	0.7984681	0.6515876	0.8292085
345	21	0.7404788	0.6824087	0.7985488	0.6516683	0.8292892
346	22	0.7404786	0.6824086	0.7985487	0.6516682	0.8292891
347	23	0.7404791	0.6824091	0.7985491	0.6516686	0.8292895
348	24	0.7404758	0.6824058	0.7985458	0.6516654	0.8292863

349 $\alpha_{2,t}$:

350	alpha2	y_lo80	y_hi80	y_lo95	y_hi95	
351	13	-1.250640	-1.351785	-1.149495	-1.405328	-1.095952
352	14	-1.243294	-1.344439	-1.142149	-1.397982	-1.088606
353	15	-1.241429	-1.342574	-1.140284	-1.396117	-1.086741
354	16	-1.243868	-1.345014	-1.142723	-1.398557	-1.089180
355	17	-1.244483	-1.345628	-1.143338	-1.399171	-1.089795
356	18	-1.241865	-1.343010	-1.140719	-1.396553	-1.087177
357	19	-1.240814	-1.341959	-1.139669	-1.395502	-1.086126
358	20	-1.240371	-1.341516	-1.139226	-1.395059	-1.085683
359	21	-1.240237	-1.341382	-1.139092	-1.394925	-1.085549
360	22	-1.240276	-1.341421	-1.139131	-1.394964	-1.085588
361	23	-1.240329	-1.341474	-1.139184	-1.395017	-1.085641
362	24	-1.240308	-1.341453	-1.139163	-1.394996	-1.085620

363 $\alpha_{3,t}$:

364	alpha3	y_lo80	y_hi80	y_lo95	y_hi95	
365	13	4.584836	4.328843	4.757406	4.215410	4.870840
366	14	4.546167	4.307253	4.849862	4.163634	4.993482
367	15	4.527651	4.201991	4.803004	4.042913	4.962082
368	16	4.513810	4.216525	4.850160	4.048812	5.017874
369	17	4.517643	4.176214	4.828735	4.003502	5.001446
370	18	4.523109	4.203064	4.866713	4.027406	5.042371
371	19	4.522772	4.178489	4.848760	4.001079	5.026170
372	20	4.521846	4.191833	4.866066	4.013374	5.044524
373	21	4.521382	4.177560	4.854171	3.998472	5.033259
374	22	4.521451	4.186714	4.864755	4.007248	5.044222
375	23	4.521772	4.178995	4.857897	3.999300	5.037591
376	24	4.521862	4.184734	4.864155	4.004903	5.043987

377 *Appendix .2 Stressed forecast ($\alpha_{1,t} + 0.5\%$) and confidence intervals for $\alpha_{i,t}$, $i = 1, \dots, 3$ forecasts*378 $\alpha_{1,t}$:

```

379  alpha1  y_lo80  y_hi80  y_lo95  y_hi95
380  13    1.25  1.19193  1.30807  1.16119  1.33881
381  14    1.25  1.19193  1.30807  1.16119  1.33881
382  15    1.25  1.19193  1.30807  1.16119  1.33881
383  16    1.25  1.19193  1.30807  1.16119  1.33881
384  17    1.25  1.19193  1.30807  1.16119  1.33881
385  18    1.25  1.19193  1.30807  1.16119  1.33881
386  19    1.25  1.19193  1.30807  1.16119  1.33881
387  20    1.25  1.19193  1.30807  1.16119  1.33881
388  21    1.25  1.19193  1.30807  1.16119  1.33881
389  22    1.25  1.19193  1.30807  1.16119  1.33881
390  23    1.25  1.19193  1.30807  1.16119  1.33881
391  24    1.25  1.19193  1.30807  1.16119  1.33881

```

392 $\alpha_{2,t}$:

```

393  alpha2  y_lo80  y_hi80  y_lo95  y_hi95
394  13 -1.222568 -1.323713 -1.121423 -1.377256 -1.067880
395  14 -1.219401 -1.320546 -1.118256 -1.374089 -1.064713
396  15 -1.211361 -1.312506 -1.110216 -1.366049 -1.056673
397  16 -1.216213 -1.317358 -1.115068 -1.370901 -1.061525
398  17 -1.215266 -1.316411 -1.114121 -1.369954 -1.060578
399  18 -1.211474 -1.312619 -1.110329 -1.366162 -1.056786
400  19 -1.210329 -1.311474 -1.109183 -1.365017 -1.055640
401  20 -1.209610 -1.310755 -1.108465 -1.364298 -1.054922
402  21 -1.209648 -1.310793 -1.108503 -1.364336 -1.054960
403  22 -1.209601 -1.310746 -1.108456 -1.364289 -1.054913
404  23 -1.209688 -1.310833 -1.108542 -1.364376 -1.055000
405  24 -1.209653 -1.310798 -1.108508 -1.364341 -1.054965

```

406 $\alpha_{3,t}$:

```

407  alpha3  y_lo80  y_hi80  y_lo95  y_hi95
408  13  4.500390  4.244398  4.672961  4.130964  4.786394
409  14  4.482948  4.244035  4.786643  4.100415  4.930263
410  15  4.441841  4.116182  4.717194  3.957103  4.876272
411  16  4.441744  4.144459  4.778094  3.976746  4.945808
412  17  4.439609  4.098181  4.750701  3.925469  4.923413
413  18  4.447151  4.127105  4.790755  3.951448  4.966412
414  19  4.446164  4.101881  4.772152  3.924471  4.949562
415  20  4.445421  4.115407  4.789641  3.936949  4.968099
416  21  4.445411  4.101589  4.778200  3.922501  4.957289
417  22  4.445491  4.110754  4.788795  3.931287  4.968262
418  23  4.445937  4.103160  4.782062  3.923465  4.961756
419  24  4.446012  4.108885  4.788306  3.929053  4.968137

```

420 *Appendix .3 Out-of-sample log(RMSE) as a function of $\log(\lambda_1)$ and $\log(\lambda_2)$*

```

421  log_lambda1  log_lambda2  log_error
422  1          -4.605170    -4.605170  13.5039336
423  2          -3.070113    -4.605170  14.3538621
424  3          -1.535057    -4.605170  14.7912525
425  4           0.000000    -4.605170  14.8749375

```

426	5	1.535057	-4.605170	14.8928025
427	6	3.070113	-4.605170	14.8962203
428	7	4.605170	-4.605170	14.8975776
429	8	6.140227	-4.605170	14.8976494
430	9	7.675284	-4.605170	14.8976630
431	10	9.210340	-4.605170	14.8976715
432	11	-4.605170	-3.070113	3.9701229
433	12	-3.070113	-3.070113	4.9644144
434	13	-1.535057	-3.070113	5.2607788
435	14	0.000000	-3.070113	5.3208833
436	15	1.535057	-3.070113	5.3326856
437	16	3.070113	-3.070113	5.3351784
438	17	4.605170	-3.070113	5.3357136
439	18	6.140227	-3.070113	5.3358306
440	19	7.675284	-3.070113	5.3358557
441	20	9.210340	-3.070113	5.3358610
442	21	-4.605170	-1.535057	3.6692928
443	22	-3.070113	-1.535057	3.5643607
444	23	-1.535057	-1.535057	3.5063072
445	24	0.000000	-1.535057	3.4942438
446	25	1.535057	-1.535057	3.4904354
447	26	3.070113	-1.535057	3.4881352
448	27	4.605170	-1.535057	3.4888202
449	28	6.140227	-1.535057	3.4880668
450	29	7.675284	-1.535057	3.4886911
451	30	9.210340	-1.535057	3.4886383
452	31	-4.605170	0.000000	3.6224691
453	32	-3.070113	0.000000	3.8313407
454	33	-1.535057	0.000000	3.8518759
455	34	0.000000	0.000000	3.8163287
456	35	1.535057	0.000000	3.7993471
457	36	3.070113	0.000000	3.7948073
458	37	4.605170	0.000000	3.7937787
459	38	6.140227	0.000000	3.7935546
460	39	7.675284	0.000000	3.7935063
461	40	9.210340	0.000000	3.7934958
462	41	-4.605170	1.535057	-1.2115597
463	42	-3.070113	1.535057	-1.0130537
464	43	-1.535057	1.535057	-0.5841784
465	44	0.000000	1.535057	-0.3802817
466	45	1.535057	1.535057	-0.3109827
467	46	3.070113	1.535057	-0.2931830
468	47	4.605170	1.535057	-0.2891586
469	48	6.140227	1.535057	-0.2882824
470	49	7.675284	1.535057	-0.2880932
471	50	9.210340	1.535057	-0.2880524
472	51	-4.605170	3.070113	-2.0397856
473	52	-3.070113	3.070113	-3.1729003
474	53	-1.535057	3.070113	-3.8655596
475	54	0.000000	3.070113	-3.9279840

476	55	1.535057	3.070113	-3.9508440
477	56	3.070113	3.070113	-4.0270316
478	57	4.605170	3.070113	-4.0831569
479	58	6.140227	3.070113	-4.0953167
480	59	7.675284	3.070113	-4.0979447
481	60	9.210340	3.070113	-4.0985113
482	61	-4.605170	4.605170	-2.6779260
483	62	-3.070113	4.605170	-3.4704808
484	63	-1.535057	4.605170	-4.0404935
485	64	0.000000	4.605170	-4.2441836
486	65	1.535057	4.605170	-4.3657802
487	66	3.070113	4.605170	-4.3923094
488	67	4.605170	4.605170	-4.3862826
489	68	6.140227	4.605170	-4.3830293
490	69	7.675284	4.605170	-4.3820703
491	70	9.210340	4.605170	-4.3818486
492	71	-4.605170	6.140227	-3.5007058
493	72	-3.070113	6.140227	-3.8389274
494	73	-1.535057	6.140227	-4.1969545
495	74	0.000000	6.140227	-4.3400025
496	75	1.535057	6.140227	-4.4179718
497	76	3.070113	6.140227	-4.3797034
498	77	4.605170	6.140227	-4.3073100
499	78	6.140227	6.140227	-4.2866647
500	79	7.675284	6.140227	-4.2820357
501	80	9.210340	6.140227	-4.2810151
502	81	-4.605170	7.675284	-3.7236774
503	82	-3.070113	7.675284	-4.0057353
504	83	-1.535057	7.675284	-4.2699684
505	84	0.000000	7.675284	-4.3569254
506	85	1.535057	7.675284	-4.4156364
507	86	3.070113	7.675284	-4.3842360
508	87	4.605170	7.675284	-4.2759516
509	88	6.140227	7.675284	-4.2425876
510	89	7.675284	7.675284	-4.2346514
511	90	9.210340	7.675284	-4.2328863
512	91	-4.605170	9.210340	-3.7706268
513	92	-3.070113	9.210340	-4.0406387
514	93	-1.535057	9.210340	-4.2776907
515	94	0.000000	9.210340	-4.3498230
516	95	1.535057	9.210340	-4.4095778
517	96	3.070113	9.210340	-4.3860089
518	97	4.605170	9.210340	-4.2647179
519	98	6.140227	9.210340	-4.2273624
520	99	7.675284	9.210340	-4.2183911
521	100	9.210340	9.210340	-4.2163638

522 **References**

- 523 Bergmeir, C., R. J. Hyndman, B. Koo, et al.. 2015. A note on the validity of cross-validation for evaluating time
524 series prediction. *Monash University, Department of Econometrics and Business Statistics, Tech. Rep.*
- 525 Bonnin, F., F. Combes, F. Planchet, and M. Tammar. 2015. Un modèle de projection pour des contrats de retraite
526 dans le cadre de l'orsca. *Bulletin Français d'Actuariat* 14, 107–129.
- 527 Boyle, P. P. and K. S. Tan. 1997. Quasi-monte carlo methods. In *International AFIR Colloquium Proceedings, Australia*,
528 Volume 1, pp. 1–24.
- 529 Caruana, R.. 1998. Multitask learning. In *Learning to learn*, pp. 95–133. Springer.
- 530 Chakraborty, K., K. Mehrotra, C. K. Mohan, and S. Ranka. 1992. Forecasting the behavior of multivariate time
531 series using neural networks. *Neural networks* 5(6), 961–970.
- 532 Cormen, T. H.. 2009. *Introduction to algorithms*. MIT press.
- 533 Dehuri, S. and S.-B. Cho. 2010. A comprehensive survey on functional link neural networks and an adaptive
534 pso-bp learning for cflnn. *Neural Computing and Applications* 19(2), 187–205.
- 535 Diebold, F. X. and C. Li. 2006. Forecasting the term structure of government bond yields. *Journal of*
536 *econometrics* 130(2), 337–364.
- 537 Diebold, F. X. and G. D. Rudebusch. 2013. *Yield Curve Modeling and Forecasting: The Dynamic Nelson-Siegel Approach*.
538 Princeton University Press.
- 539 Dutang, C. and P. Savicky. 2015. *randtoolbox: Generating and Testing Random Numbers*. R package version 1.17.
- 540 Exterkate, P., P. J. Groenen, C. Heij, and D. van Dijk. 2016. Nonlinear forecasting with many predictors using
541 kernel ridge regression. *International Journal of Forecasting* 32(3), 736–753.
- 542 Hochreiter, S. and J. Schmidhuber. 1997. Long short-term memory. *Neural computation* 9(8), 1735–1780.
- 543 Hoerl, A. E. and R. W. Kennard. 1970. Ridge regression: Biased estimation for nonorthogonal problems.
544 *Technometrics* 12(1), 55–67.
- 545 Hyndman, R. J. and Y. Khandakar. 2008. Automatic time series forecasting: The forecast package for r. *Journal of*
546 *Statistical Software* 27(i03).
- 547 Joe, S. and F. Kuo. 2008. Notes on generating sobol sequences. <http://web.maths.unsw.edu.au/~fkuo/sobol/joe-kuo-notes.pdf>.
- 548
- 549 Lütkepohl, H.. 2005. *New introduction to multiple time series analysis*. Springer Science & Business Media.
- 550 Nelson, C. R. and A. F. Siegel. 1987. Parsimonious modeling of yield curves. *Journal of business*, 473–489.
- 551 Niederreiter, H.. 1992. *Random number generation and quasi-Monte Carlo methods*. SIAM.
- 552 Pankratz, A.. 2012. *Forecasting with dynamic regression models*, Volume 935. John Wiley & Sons.
- 553 Pao, Y.-H., G.-H. Park, and D. J. Sobajic. 1994. Learning and generalization characteristics of the random vector
554 functional-link net. *Neurocomputing* 6(2), 163–180.
- 555 Penrose, R.. 1955. A generalized inverse for matrices. In *Mathematical proceedings of the Cambridge philosophical*
556 *society*, Volume 51, pp. 406–413. Cambridge Univ Press.
- 557 Pfaff, B. et al.. 2008. Var, svar and svec models: Implementation within r package vars. *Journal of Statistical*
558 *Software* 27(4), 1–32.
- 559 Ren, Y., P. Suganthan, N. Srikanth, and G. Amaratunga. 2016. Random vector functional link network for
560 short-term electricity load demand forecasting. *Information Sciences* 367, 1078–1093.
- 561 Rumelhart, D., G. Hinton, and R. Williams. 1988. Learning internal representations by error propagation. In
562 *Neurocomputing: foundations of research*, pp. 673–695. MIT Press.
- 563 Schmidt, W. F., M. A. Kraaijeveld, and R. P. Duin. 1992. Feedforward neural networks with random weights. In
564 *Pattern Recognition, 1992. Vol. II. Conference B: Pattern Recognition Methodology and Systems, Proceedings., 11th*
565 *IAPR International Conference on*, pp. 1–4. IEEE.
- 566 Wickham, H.. 2016. *ggplot2: elegant graphics for data analysis*. Springer.
- 567 Zhang, L. and P. Suganthan. 2016. A comprehensive evaluation of random vector functional link networks.
568 *Information Sciences* 367, 1094–1105.